

Rabi frequency for polar systems interacting with light

Piotr Gladysz* and Karolina Slowik†

*Institute of Physics, Faculty of Physics, Astronomy and Informatics,
Nicolaus Copernicus University in Toruń, Grudziadzka 5/7, 87-100 Toruń, Poland*

We investigate the dynamics of polar systems coupled to classical external beams in the ultrastrong coupling regime. The permanent dipole moments (PDMs) sustained by polar systems can couple to the electromagnetic field, giving rise to a variety of processes such as difference-frequency and harmonic generation, reflected in complicated dynamics of the atomic system. Here, we demonstrate that the dynamics can be described simply in a dynamic reference frame. We derive a Jaynes–Cummings-like framework with effective parameters describing frequency shift, coupling strength with the driving field, and a rescaled relaxation rate. The familiar linear scaling of the interaction strength with the field amplitude is replaced with a nonlinear dependence, suggesting potential applications for improving the coherence of quantum system ensembles with permanent dipoles.

The interaction of light with matter is a fundamental phenomenon in physics, which underpins many modern quantum optics and photonics [1–4]. Polar systems, characterized by the presence of the PDMs due to the lack of inversion symmetry, offer unique opportunities and challenges in this domain [5–9]. Unlike transition dipole moments that occur between pairs of system eigenstates, permanent dipoles are inherent properties of individual eigenstates and can significantly influence the system’s response to external electromagnetic fields [10–15].

Traditionally, the role of permanent dipoles in light-matter interaction has been considered minor, often relegated to causing trivial frequency shifts. However, recent studies have shown that these dipoles can induce coherent radiation at the Rabi frequency, leading to more complex and rich dynamical behaviors than previously understood [10, 14, 16]. Polar systems have been suggested for lasing at tunable frequencies [12], radiation generation in tailored photonic environments [17, 18], efficient two-photon excitation [16, 19] and light squeezing [11, 13]. Materials with inherent $\chi^{(2)}$ nonlinearity were proposed for difference-frequency generation in a related mechanism [20]. Similar effects were also studied in the magnetic context, where a rescaling of the Landé g factor was found in atoms dressed with radiofrequency magnetic fields [21].

In this manuscript, we investigate the dynamics of polar systems in the ultrastrong coupling regime with external beams, where the interaction strength between the electromagnetic field and the system is comparable to or exceeds the transition frequency of the system itself [22]. Despite the variety of processes that can occur in this regime, we reveal, through a series of unitary operations rotating the reference frame, that the system’s behavior can be elegantly captured using a Jaynes–Cummings-type analytically solvable model. This description, set in a dynamic reference frame, is based on three key parameters: the rescaled frequency shift, coupling strength, and the relaxation rate. The rescaling is a qualitative change: For example, the traditional linear dependence of interaction strength with the driving field amplitude is replaced

by a nonlinear one, suggesting new potential regimes for the exploration of light-matter interactions. We thoroughly verify the applicability range of the effective analytical description, confirming the robustness and accuracy of the model up to the ultrastrong coupling, where it shows good agreement with the full Hamiltonian dynamics but significantly reduces the computational cost. Finally, based on the effective Hamiltonian, we find analytical expressions for resonance fluorescence spectra that would otherwise be challenging to access, due to the involvement of processes occurring at time scales that may differ by orders of magnitude, making the numerical integration challenging.

We consider a two-level polar quantum system (TLS) with the excited $|e\rangle$ and ground $|g\rangle$ states separated with the transition frequency ω_{eg} . It is subject to a classical plane-wave laser drive $\vec{E}(t) = \vec{E}_0 \cos(\omega_c t)$ with the amplitude \vec{E}_0 and frequency $\omega_c \approx \omega_{eg}$ near-resonant with the system transition. For a polar system, light couples with the full dipole moment $\vec{d} = \sum_{ij} \vec{d}_{ij} |i\rangle \langle j|$ with $i, j \in \{e, g\}$, which includes the transition $\vec{d}_{i \neq j}$ and permanent \vec{d}_{ii} elements. The Hamiltonian reads

$$\begin{aligned} H(t)/\hbar &= \frac{1}{2} \omega_{eg} \sigma_z + \vec{E}(t) \cdot \vec{d} \\ &= \frac{1}{2} \underbrace{(\omega_{eg} + g_z \cos(\omega_c t))}_{\omega_{eg}(t)} \sigma_z + g_x \cos(\omega_c t) \sigma_x \end{aligned} \quad (1)$$

Here, $\sigma_{x,z}$ are standard Pauli matrices. The drive induces transitions between the eigenstates with the strength $g_x = \vec{E}_0 \vec{d}_{eg} / \hbar$, and a sinusoidal energy shift with the amplitude $g_z = \vec{E}_0 \Delta \vec{d} / \hbar$, where $\Delta \vec{d} = \vec{d}_{ee} - \vec{d}_{gg}$. Although the g_x term also occurs in the standard nonpolar case, the term proportional to g_z is unique to systems with PDMs and is key to the effects investigated in this work. To quantify its impact, we introduce a parameter $\kappa_z = g_z / \omega_c$ which reduces to 0 for nonpolar systems and is of the order of 1 for polar systems in the ultrastrong coupling regime, in which the dynamics is qualitatively altered.

A nonpolar system driven by light undergoes Rabi pop-

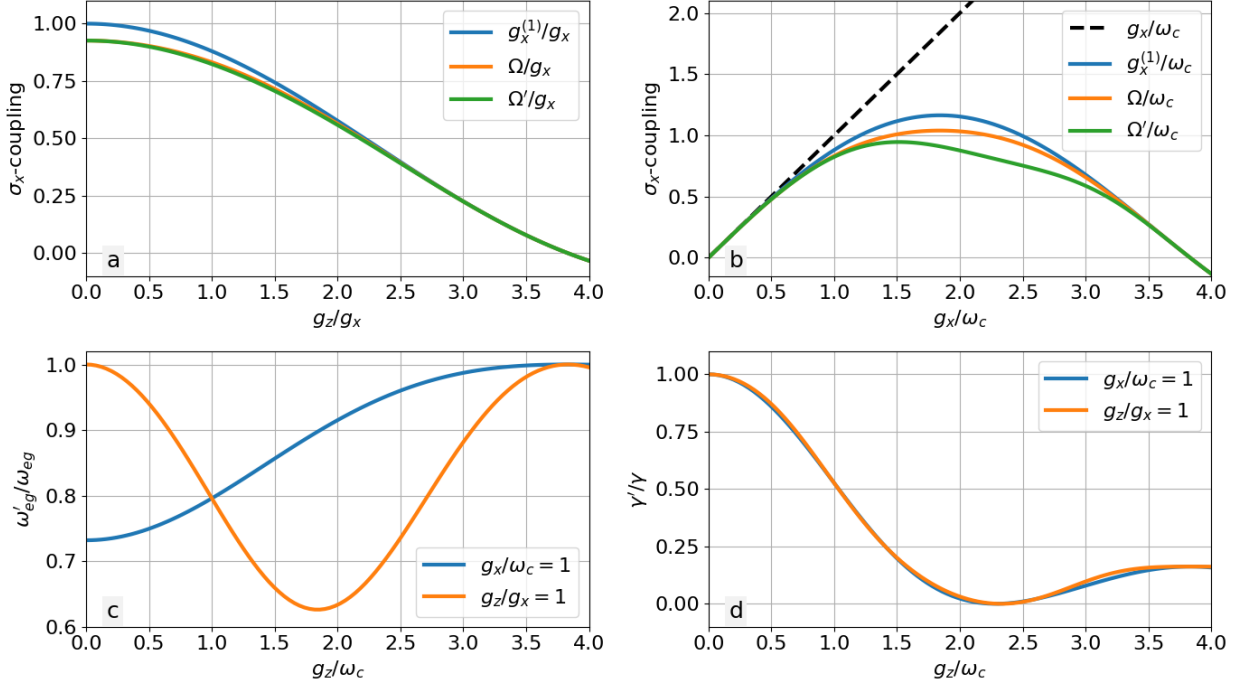


FIG. 1. The upper plots show comparisons of the $\hat{\sigma}_x$ -coupling strengths for different corrections as a function of: **a.** PDMs difference (for $g_x/\omega_c = 1$), **b.** driving field amplitude (for $g_z/\omega_c = 1$). The lower plots present: **c.** the normalized effective transition frequency, **d.** the normalized effective gamma rate, as functions of g_z coupling, both in cases of fixed driving field (blue) or PDMs difference (orange), respectively.

ulation oscillations with the Rabi frequency that for weak relaxation is given by $\Omega_R \approx \sqrt{|g_x|^2 + \delta^2}$, and depends on the drive amplitude and detuning $\delta = \omega_c - \omega_{eg}$ [23]. In a polar system, the eigenstate energies oscillate inducing a time-dependent detuning according to Eq. (1) $\delta(t) = \delta + g \cos \omega_c t$, leading to complicated dynamics mixing a range of oscillation frequencies. In the ultrastrong coupling regime, these contributions should not be neglected *a priori* through a rotating-wave-type approximation. In Supplementary Material Section I, we document in detail a transition to a reference frame that allows one to capture this complicated behavior in an analytically solvable model. The transition involves a series of noncommutative reference frame rotations. These rotations subsequently simplify the form of the Hamiltonian. With the first transformation $U_1 = \exp(\frac{1}{2}i\kappa_z \sin(\omega_c t)\sigma_z)$, the terms proportional to g_z are incorporated in the parameters of an effective Rabi-like model,

$$H_1/\hbar = \frac{1}{2}\omega_{eg}\sigma_z + g_x^{(1)}\sigma_x \cos \omega_c t + H_{\text{multi}}/\hbar, \quad (2)$$

corrected by higher-order terms H_{multi} related to resonances at $n\omega_c = \omega_{eg}$, $n \geq 2$ [Supplementary Material Eq. (S7)] which can be associated with multiphoton processes. The coupling constant describing effects resonant

at $n\omega_c$ is given by

$$g_x^{(n)}(\vec{E}_0, \vec{d}_{eg}, \Delta\vec{d}, \omega_c) \equiv g_x^{(n)}(\kappa_z) = \frac{2n}{\kappa_z} J_n(\kappa_z) g_x, \quad (3)$$

where $J_n(x)$ is the n th-order Bessel function of the first kind. This step involves no approximations and the polar terms are fully included. However, in a frame rotating with a sinusoidally varying frequency, the system behaves as if it were not polar but coupled with an electromagnetic field through a modified coupling strength $g_x^{(1)}$, nonlinearly dependent on the field amplitude. As we verify in Fig. 5, the corrections arising from H_{multi} may become important for the case of the ultrastrong σ_x -coupling.

In the following steps, counter-rotating terms are similarly incorporated in effective parameters through the pair of transformations $U_2 = \exp(i\xi\kappa_x \sin(\omega_c t)\sigma_x)$ [24] and $U_3 = \exp(\frac{1}{2}i\kappa'_z \sin(\omega_c t)\sigma_z)$. Here, $\kappa_x = g_x^{(1)}/\omega_c$, and κ'_z is a cumbersome function of dipole moment elements and the driving field, defined in the Supplementary Material Section I. The parameter $\xi \in (0, 1)$ fulfills the equation [24]

$$\omega_{eg} J_1(2\xi\kappa_x) = (1 - \xi)g_x^{(1)} \equiv \frac{1}{2}\Omega, \quad (4)$$

where Ω plays the role of an effective coupling strength

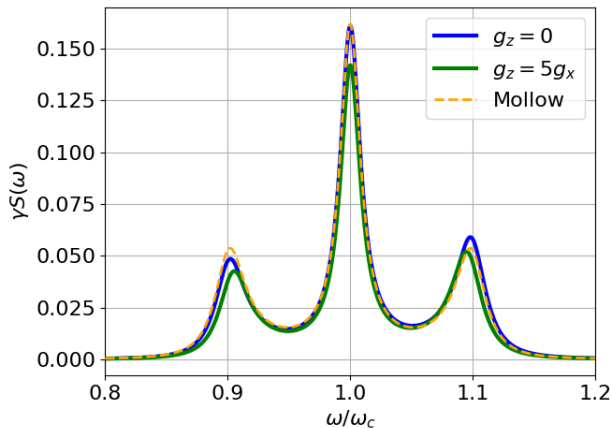


FIG. 2. Comparison of spectra calculated for the two-level system with (green line), and without (blue line) PDMs, and the Mollow-triplet (dashed line), calculated for the resonant case $\omega_c = \omega_{eg}$. The coupling strength $g_x/\omega_c = 0.1$ and the relaxation rates $\gamma/\omega_c = \gamma'/\omega_c = 0.02$ were assumed to be the same for all cases. In the polar case, $g_z = 5g_x$.

obtained in the intermediate step. The resulting Hamiltonian has the Jaynes–Cummings form as it occurs in the Schrödinger-picture. The transformation $U_4 = \exp(\frac{1}{2}i\omega_c t \sigma_z)$ brings it to the interaction picture, where it is time-independent and acquires the final analytically solvable form

$$H_{\text{eff}}/\hbar = -\frac{1}{2}\delta'\sigma_z + \frac{1}{2}\Omega'\sigma_x. \quad (5)$$

Here, we have omitted multiphoton corrections negligible in the regime investigated below. The Hamiltonian (5) is analytically solvable, and yet, accounts for a plethora of physical effects related to the system’s asymmetry *via* PDMs, ultrastrong coupling, Bloch–Siegert shift, and beyond, and is exact up to multiphoton effects. The rich variety of the captured phenomena is reflected in the effective parameters that we now discuss. The field detuning $\delta' = \omega_c - \omega'_{eg}$ is defined with respect to the effective transition frequency $\omega'_{eg} = \omega_{eg}J_0(2\xi\kappa_x)$, whose dominant Taylor expansion coefficient

$$\xi^2\omega_{eg}\frac{J_1(\kappa_z)^2|2g_x|^2}{\kappa_z^2\omega_c^2} \xrightarrow{\kappa_z \rightarrow 0} \xi^2\omega_{eg}|g_x|^2\omega_c^2$$

can be recognized as the Bloch–Siegert shift [25]. The scaling of the effective frequency ω'_{eg} with normalized g_z coupling is shown in Fig. 1(c).

The effective coupling strength has a complicated functional dependence on the field amplitude and atomic dipole moments

$$\Omega' = J_0(\kappa'_z)\Omega \approx g_x^{(1)}. \quad (6)$$

where the latter approximate expression is valid for moderately strong interactions with $\vec{E}_0\Delta\vec{d} < \hbar\omega_c$. Therefore,

we have found an iterative sequence of coupling strengths $g_x^{(1)} \rightarrow \Omega \rightarrow \Omega'$ obtained through subsequent rotations. The effective coupling strengths are plotted in Fig. 1(a,b) respectively as a function of the PDMs difference in the TLS eigenstates and of the electric field amplitude. The blue, orange, and green lines represent coupling strengths after subsequent frame rotations, and the black dashed line is the usual coupling strength linearly scaled with the field amplitude in the original reference frame.

To account for dissipative dynamics, we have augmented the Hamiltonian (1) with a coupling to a bosonic thermal bath and performed the same reference frame rotations. These steps are described in detail in Supplementary Material Section II. As a result, following the Weisskopf–Wigner theory with the Markovian approximation, we find a rescaled spontaneous emission rate which for $\vec{E}_0\Delta\vec{d} \leq \hbar\omega_c$ takes the approximate form

$$\gamma' \approx J_0(\kappa_z)^2 J_0(\kappa'_z)^2 \gamma, \quad (7)$$

and is further modified for strong fields (see Supplementary Material Section II for exact formulas). Thus, in the dynamic frame, the spontaneous emission rate in polar systems depends on the external field amplitude E_0 [see Fig. 1(d), where the rate is shown without approximations]. The emission rate keeps its original value γ for vanishing PDMs or in the absence of an external field.

The simple form of the effective Hamiltonian (5) allows us to analytically evaluate the stationary expectation values of the population inversion and the induced dipole moment in the rotated frame, as derived in Supplementary Material Section III

$$\langle\sigma^\pm\rangle_s = \frac{\Omega'(2\delta' \pm i\gamma')}{2\Omega'^2 + 4\delta'^2 + \gamma'^2}, \quad (8a)$$

$$\langle\sigma_z\rangle_s = -\frac{(4\delta'^2 + \gamma'^2)}{2\Omega'^2 + 4\delta'^2 + \gamma'^2}. \quad (8b)$$

Building upon stationary solutions, we use the Onsager–Lax theorem to evaluate the fluorescence spectrum of the system following the approach proposed by [24] for nonpolar systems. At this step, the price for the simplicity of the Hamiltonian is the complicated form of the evolution operator in the rotating frame that makes the resulting expressions quite complex. Yet, we obtain their analytical forms predicting a sequence of Mollow triplets centered at multiples $n\omega_c$ of the illumination frequency, with sidebands separated by the effective Rabi frequency $\tilde{\Omega}$, which is calculated based on the coupling strength Ω' and γ' -rate such that $\tilde{\Omega} \rightarrow \Omega'$ for $\gamma' \rightarrow \gamma$. For the full derivation of the lineshapes and $\tilde{\Omega}$ parameter see Supplementary Material Section IV.

Let us first analyze the resulting spectrum of a polar system illuminated at $\omega_c = \omega_{eg}$ around the original peak, i.e., in the vicinity of the illumination frequency. This result is compared with the one obtained for the non-polar

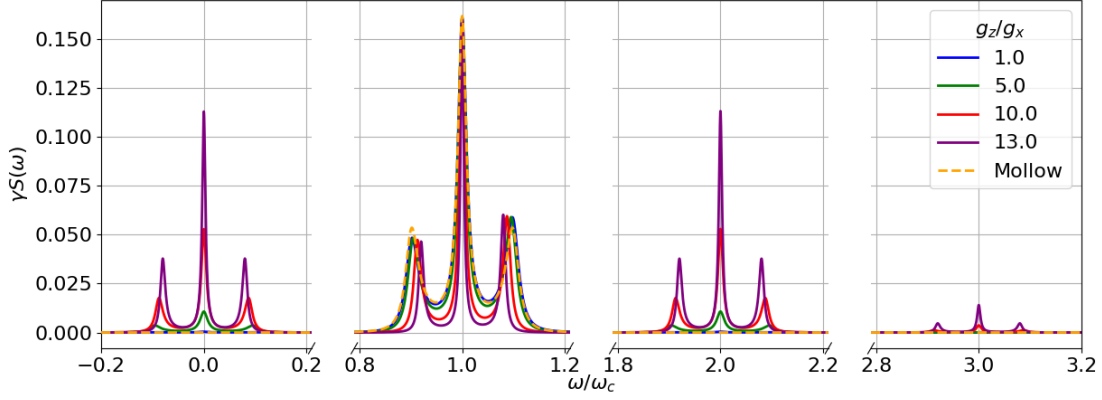


FIG. 3. Comparison of spectra for several different values of the PDMs (g_z/g_x ratios) and compared to the results obtained by Mollow (dashed line), obtained for the resonant case $\omega_c = \omega_{eg}$, $\gamma/\omega_c = 0.02$, $g_x/\omega_{eg} = 0.1$. In the plot, calculated γ' values are used.

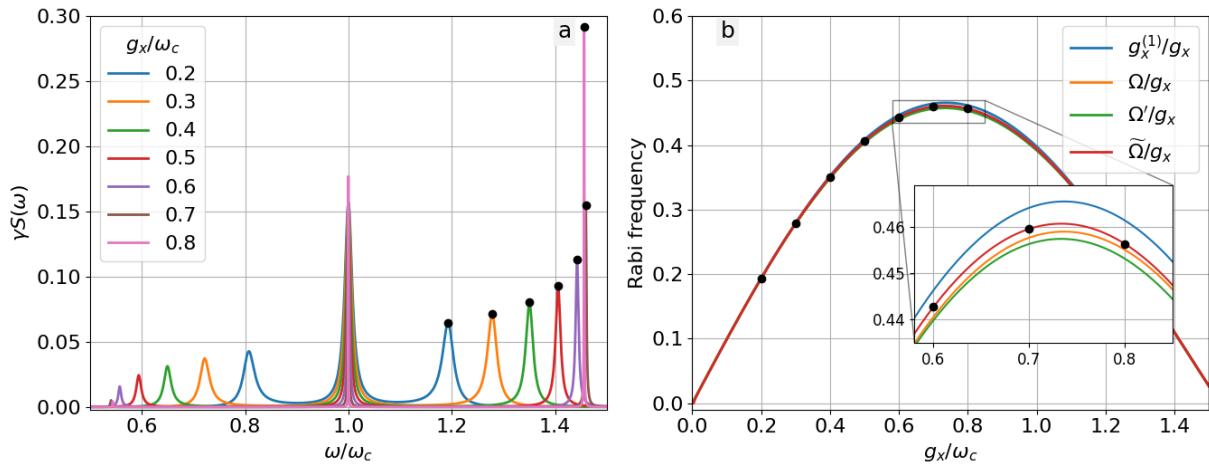


FIG. 4. **a.** Resonance fluorescence spectra for different values of the $\hat{\sigma}_x$ -coupling g_x and fixed PDMs difference $g_z/g_x = 2.5$. For each spectrum $\omega_c = \omega_{eg}$, and spontaneous emission rates γ 's are calculated based on $\gamma/\omega_c = 0.02$. **b.** Position of the peaks of the right sidebands shown on top of the curves with approximations to the evaluation of the Rabi frequency.

case [24] and the analytical results derived by Mollow [26] (Fig. 2). The relatively strong field, and hence the significant correction to the atomic frequency and nonzero effective detuning are responsible for the asymmetry of the sidebands in both polar and nonpolar cases but are not captured by the Mollow solution. This asymmetry is comparable in the two former cases, hence we conclude that the existence of the PDMs does not impact significantly the resonance shift. However, it is crucial for the correct evaluation of the peak amplitudes and spectral positions of the sidebands, given by the effective coupling $\tilde{\Omega}$.

We now proceed to discuss the spectral features centered at $n\omega_c$. Neglecting multiphoton corrections, the

relevant terms correspond to $n = 0, 1, 2, 3$, as predicted in earlier studies [15]. In systems without PDMs, the emission at even multiples of the laser frequency does not occur [16]. The peak at $3\omega_{eg}$ is induced in this case by the counter-rotating terms in the Rabi Hamiltonian [15, 27]. Polarity in the system reduces the Hamiltonian symmetry, gives rise to the even-order fluorescence peaks, and modifies the odd ones. The low-energy emission at Rabi frequency $\tilde{\Omega}$ discussed previously in various contexts [10, 12, 14], is captured here as the Mollow sideband of the triplet corresponding to $n = 0$. In Fig. 3, we demonstrate the spectra for $g_x/\omega_c = 0.1$ and $g_z/\omega_c = 0.1, 0.5, 1.0$ and 1.3 . We assume the laser is tuned to the original atomic resonance $\omega_c = \omega_{eg}$. Again, the field gives

rise to a large frequency shift, hence, a significant effective detuning responsible for the asymmetry of the sidebands. With increasing PDMs difference, the light interaction with the atomic system becomes dominated by related terms, in the original Hamiltonian proportional to g_z . This is reflected in the emission spectrum through the modified relative intensity of the peaks: The original Mollow triplet at ω_c , dominant for weakly polar systems with small PDMs, is gradually suppressed as the emission is directed to other frequency channels.

Finally, Fig. 4(a) shows how the spectral position of the sidebands can be tuned with the driving field amplitude. Here, we assume again the illumination at $\omega_c = \omega_{eg}$. The ratio of permanent- and transition-dipole moment element components parallel to the field is equivalent to the ratio of coupling constants, that we fix at $g_z/g_x = 2.5$. The relaxation rate is evaluated according to Eq. (7) with $\gamma/\omega_c = 0.02$. We find that as the field amplitude increases, the sidebands are initially pulled away from the central peak at a decreasing pace and eventually turn back towards the center at ω_c . Additionally, by increasing the field amplitude we decrease both the transition frequency ω' and spontaneous emission γ' -rates according to the results from Fig. 1(a,b). As a result, we observe the narrowing and growth (shrinking) of the right (left) sidebands.

In the Jaynes–Cummings model, the difference in the spectral position of the sideband and the central peak corresponds to the coupling strength. Naturally, the same is expected from the effective description that we have reduced to the Jaynes–Cummings form. Indeed, as can be seen in Fig. 4(b), the position of spectral sidebands given by $\tilde{\Omega}$ is in good agreement with the prediction of the effective coupling strength Ω' . For comparison, we also show the coupling strengths' predictions evaluated after subsequent transformations $U_1 - U_4$. As it is clear from the inset, all frame rotations need to be performed to eventually obtain the excellent agreement of $\tilde{\Omega}$ (red line) with the calculated spectral positions of sidebands (black dots). However, already the first transformation provides a qualitatively correct expression for the effective coupling strength $g_x^{(1)}$, as can be concluded from the examination of the blue line.

We aim to comment on the applicability of the derived model in Fig. 5. Each panel corresponds to a selected spectrum from Fig. 4a for a fixed value of g_x/ω_c and $g_z = 2.5g_x$ (matching colors are used). Note that for $g_x/\omega_c = 0.4$, ultra-strong σ_z -coupling is already reached with $g_z = \omega_c$. Despite the simplicity of the effective Hamiltonian described with a pair of effective parameters, we obtain very good agreement with the full Hamiltonian dynamics even near the Bessel function peak. We can thus capture the complex dynamics of systems with permanent dipoles subjected to extremely strong electromagnetic fields with this simple model. Beyond

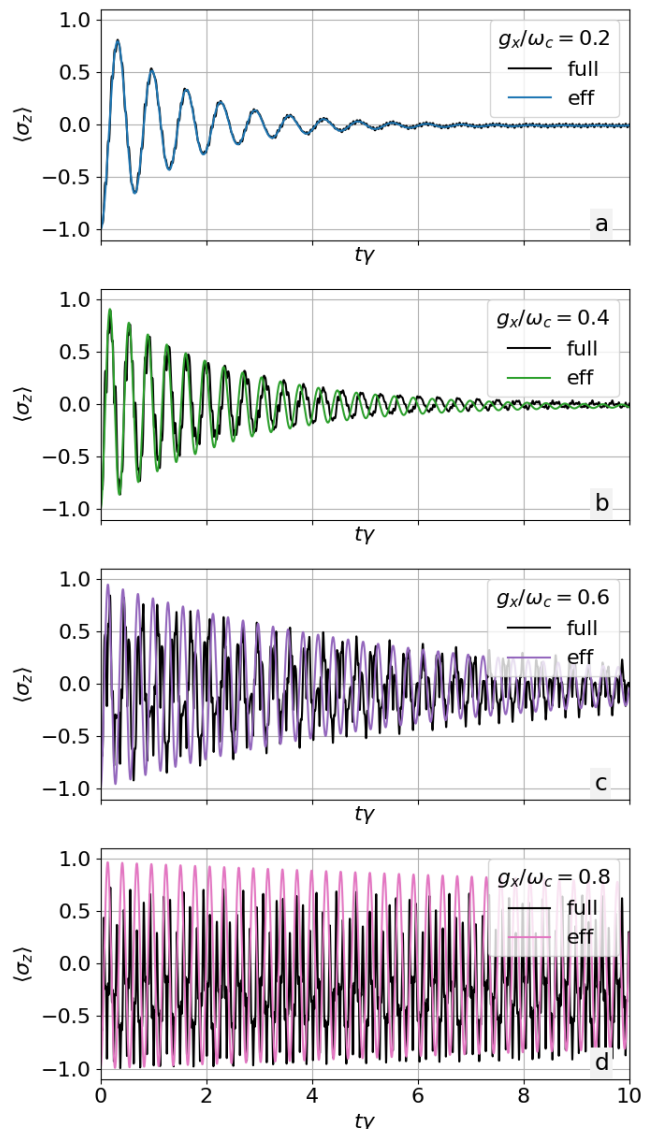


FIG. 5. Evolution of the population represented by $\langle \hat{\sigma}_z \rangle$. Each plot corresponds to one of the spectral lineshapes presented in Fig. 4a (color matching),

$g_x/\omega_c = 0.6$ [Fig. 5(c)], multiphoton corrections begin to play a more important role so that the effective dynamics ceases to predict the qualitative behaviour of the system. Moreover, in this regime the suppression of the γ' -rate is significant and in Fig. 5(c,d) leads to the reduction of the oscillations' damping. The involvement of the multiphoton corrections could also alter this behavior.

In conclusion, we explored the behavior of polar systems under ultrastrong coupling with classical external beams. By switching to a dynamic reference frame using a series of unitary operations, we derived an analytically solvable Jaynes–Cummings-like model. This model captures the impact of PDMs, counter-rotating terms, and strong fields in effective frequency shift, coupling

strengths, and relaxation rate, helping us understand the complex interactions in these systems.

Our findings show that permanent dipoles play a crucial role in changing how the system interacts with external fields, leading to a nonlinear interaction strength. This shift from traditional linear scaling suggests new avenues for research on light interactions with polar matter, especially in enhancing the coherence of multiple quantum systems with permanent dipoles. Future research should investigate the identified nonlinear effects and their practical applications, explore more complex quantum systems, and study their behavior under different external conditions. Additionally, expanding this framework to include multiphoton interactions and multipartite dynamics could offer further insights into the principles that govern this interesting interaction regime.

Acknowledgement: The authors acknowledge the support from the National Science Centre, Poland, PRELUDIUM programme (grant number 2021/41/N/ST2/02068).

* glad@doktorant.umk.pl

† karolina@fizyka.umk.pl

- [1] D. Dovzhenko, S. Ryabchuk, Y. P. Rakovich, and I. Nabiev, Light–matter interaction in the strong coupling regime: configurations, conditions, and applications, *Nanoscale* **10**, 3589 (2018).
- [2] M. Hertzog, M. Wang, J. Mony, and K. Börjesson, Strong light–matter interactions: a new direction within chemistry, *Chemical Society Reviews* **48**, 937 (2019).
- [3] N. Rivera and I. Kaminer, Light–matter interactions with photonic quasiparticles, *Nature Reviews Physics* **2**, 538 (2020).
- [4] A. Marinho, M. de Paula, and A. Dodonov, Approximate analytic solution of the dissipative semiclassical rabi model near the three-photon resonance and comparison with the quantum behavior, *Physics Letters A*, 129608 (2024).
- [5] M. A. Kmetić and W. J. Meath, Perturbative corrections to the rotating-wave approximation for two-level molecules and the effects of permanent dipoles on single-photon and multiphoton spectra, *Physical Review A* **41**, 1556 (1990).
- [6] D. DeMille, Quantum computation with trapped polar molecules, *Physical Review Letters* **88**, 067901 (2002).
- [7] S. A. Moses, J. P. Covey, M. T. Miecnikowski, D. S. Jin, and J. Ye, New frontiers for quantum gases of polar molecules, *Nature Physics* **13**, 13 (2017).
- [8] J. F. Triana and J. L. Sanz-Vicario, Polar diatomic molecules in optical cavities: Photon scaling, rotational effects, and comparison with classical fields, *The Journal of Chemical Physics* **154** (2021).
- [9] R. González-Férez, J. Shertzer, and H. Sadeghpour, Ultralong-range rydberg bimolecules, *Physical Review Letters* **126**, 043401 (2021).
- [10] O. Kibis, G. Y. Slepyan, S. Maksimenko, and A. Hoffmann, Matter coupling to strong electromagnetic fields in two-level quantum systems with broken inversion symmetry, *Physical review letters* **102**, 023601 (2009).
- [11] M. Koppenhöfer and M. Marthaler, Creation of a squeezed photon distribution using artificial atoms with broken inversion symmetry, *Physical Review A* **93**, 023831 (2016).
- [12] I. Y. Chestnov, V. A. Shahnazaryan, A. P. Alodjants, and I. A. Shelykh, Terahertz lasing in ensemble of asymmetric quantum dots, *Acs Photonics* **4**, 2726 (2017).
- [13] M. Antón, S. Maede-Razavi, F. Carreño, I. Thanopoulos, and E. Paspalakis, Optical and microwave control of resonance fluorescence and squeezing spectra in a polar molecule, *Physical Review A* **96**, 063812 (2017).
- [14] P. Gładysz, P. Wcisło, and K. Słowik, Propagation of optically tunable coherent radiation in a gas of polar molecules, *Scientific reports* **10**, 17615 (2020).
- [15] G. Scala, K. Słowik, P. Facchi, S. Pascazio, and F. V. Pepe, Beyond the rabi model: Light interactions with polar atomic systems in a cavity, *Physical Review A* **104**, 013722 (2021).
- [16] W. J. Meath and B. Jagatap, On the effects of permanent molecular dipoles in the simultaneous absorption of two photons: Full generalized rotating wave approximation versus analytical results, *The Journal of Chemical Physics* **139** (2013).
- [17] I. Savenko, O. Kibis, and I. A. Shelykh, Asymmetric quantum dot in a microcavity as a nonlinear optical element, *Physical Review A—Atomic, Molecular, and Optical Physics* **85**, 053818 (2012).
- [18] S. Izadshenas, P. Gładysz, and K. Słowik, Hybrid graphene-silver nanoantenna to control thz emission from polar quantum systems, *Optics Express* **31**, 29037 (2023).
- [19] W. J. Meath, On the optimization, and the intensity dependence, of the excitation rate for the absorption of two-photons due to the direct permanent dipole moment excitation mechanism, *AIP Advances* **6** (2016).
- [20] F. Barachati, S. De Liberato, and S. Kéna-Cohen, Generation of rabi-frequency radiation using exciton-polaritons, *Physical Review A* **92**, 033828 (2015).
- [21] C. Landré, C. Cohen-Tannoudji, J. Dupont-Roc, and S. Haroche, Anisotropie des propriétés magnétiques d’un atome habillé par des photons de rf, *Journal de Physique* **31**, 971 (1970).
- [22] P. Forn-Díaz, L. Lamata, E. Rico, J. Kono, and E. Solano, Ultrastrong coupling regimes of light-matter interaction, *Rev. Mod. Phys.* **91**, 025005 (2019).
- [23] R. Loudon, *The Quantum Theory of Light*, Oxford science publications (Clarendon Press, 1983).
- [24] Y. Yan, Z. Lü, and H. Zheng, Effects of counter-rotating-wave terms of the driving field on the spectrum of resonance fluorescence, *Physical Review A—Atomic, Molecular, and Optical Physics* **88**, 053821 (2013).
- [25] F. Bloch and A. Siegert, Magnetic resonance for nonrotating fields, *Physical Review* **57**, 522 (1940).
- [26] B. Mollow, Power spectrum of light scattered by two-level systems, *Physical Review* **188** (1969).
- [27] D. Braak, Integrability of the rabi model, *Physical Review Letters* **107**, 100401 (2011).

Supplementary Material for the Article

Rabi frequency for polar systems interacting with light

Piotr Gładysz* and Karolina Słowik†

Institute of Physics, Nicolaus Copernicus University in Toruń, Gagarina 11, 87-100 Toruń, Poland

This supplement contains derivations of equations discussed in the main text and additional results.

CONTENTS

I.	Derivation of Hamiltonian Eq.(5)	1
	A. Transformation U_1 – revealing higher-order resonances	2
	B. Transformation U_2 – dealing with counter-rotating terms	3
	C. Transformation U_3 – effectively removing the σ_z coupling	4
	D. Transformation U_4 – moving to the interaction picture	4
II.	Derivation of relaxation rate Eq. (7)	5
III.	Stationary solution	7
IV.	Fluorescence spectra	7
	References	10

In this supplement, we present detailed derivations of the Hamiltonian, relaxation rates and spectra in the transformed reference frame. We arrive at exact formulas and discuss approximations that lead to Eqs. (5) and (7) in the main article. For the readers' convenience, we fully re-introduce the notation so that all symbols are explained in this document. We also comment on the physical interpretation and consequences of subsequent mathematical steps.

I. DERIVATION OF HAMILTONIAN EQ.(5)

Our model considers a two-level polar quantum system (TLS) with orthogonal excited $|e\rangle$ and ground $|g\rangle$ states with transition frequency ω_{eg} . A classical plane wave $\vec{E}(t) = \vec{E}_0 \cos(\omega_c t)$ with amplitude \vec{E}_0 and frequency $\omega_c \approx \omega_{eg}$ is coupled to the TLS via the transition dipole moment \vec{d}_{eg} , and the permanent dipole moments (PDMs) \vec{d}_{ee} , \vec{d}_{gg} in excited and ground states, respectively. The Hamiltonian reads

$$\begin{aligned}
 H(t)/\hbar &= \frac{1}{2}\omega_{eg}\sigma_z + \vec{E}(t) \cdot \hat{d}, \\
 &= \frac{1}{2} \underbrace{(\omega_{eg} + g_z \cos(\omega_c t))}_{\omega_{eg}(t)} \sigma_z + g_x \cos(\omega_c t) \sigma_x + \frac{1}{2} g_I \cos(\omega_c t) I,
 \end{aligned} \tag{S1}$$

where $\sigma_z = |e\rangle\langle e| - |g\rangle\langle g|$ is the inversion operator, $\sigma_x = |e\rangle\langle g| + |g\rangle\langle e|$ is the transition operator, $I = |e\rangle\langle e| + |g\rangle\langle g|$ is the identity operator, $\hat{d} = \sum_{ij} \vec{d}_{ij} |i\rangle\langle j|$ for $i, j \in \{e, g\}$ is the dipole moment operator, $g_x = \vec{E}_0 \vec{d}_{eg} / \hbar$, $g_z = \vec{E}_0 (\vec{d}_{ee} - \vec{d}_{gg}) / \hbar$, and $g_I = \vec{E}_0 (\vec{d}_{ee} + \vec{d}_{gg}) / \hbar$ are the coupling strengths. Effectively, coupling to the PDMs is manifested as the modification of the transition frequency $\omega_{eg} \rightarrow \omega_{eg}(t)$.

In the next steps, we introduce a series of unitary transformations and justify approximations to simplify the Hamiltonian eventually resulting in a time-independent, Jaynes-Cummings-like form given by Eq. (5) of the main text.

* glad@umk.pl

† karolina@umk.pl

A. Transformation U_1 – revealing higher-order resonances

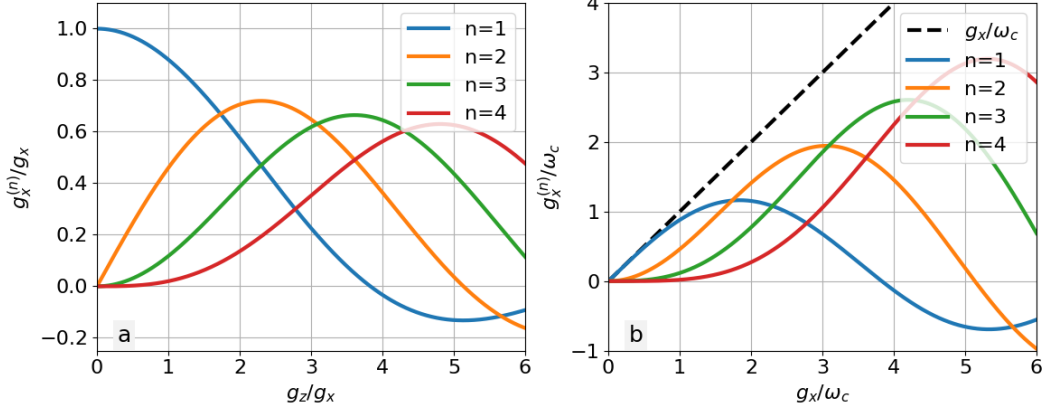


FIG. S1. Coupling strengths of single- (blue), and multi- (orange, green, red) photon resonances in two cases. **a.** As functions of PDMs difference g_z/g_x for a fixed value of the σ_x -coupling $g_x/\omega_c = 1$. and relative to g_x . **b.** As functions of the field's amplitude g_x/ω_c for a fixed value of PDMs difference $g_z/g_x = 1$. The dashed line corresponds to the nonpolar system.

First, we remove the time dependence of the term proportional to the σ_z operator using the unitary transformation proposed in this context in Ref. [1]

$$\begin{aligned} U_1 &= e^{\frac{1}{2}i\kappa_z \sin(\omega_c t)\sigma_z}, \\ U_1\sigma^\pm U_1^\dagger &= e^{\pm i\kappa_z \sin(\omega_c t)}\sigma^\pm, \end{aligned} \quad (S2)$$

where $\kappa_z = g_z/\omega_c$ is the key parameter measuring the degree of asymmetry of the system with respect to spatial inversion and reduces to 0 for non-polar systems with vanishing PDMs. The transformed Hamiltonian reads as

$$H_1/\hbar = U_1 H U_1^\dagger/\hbar + i\dot{U}_1 U_1^\dagger = \frac{1}{2}\omega_{eg}\sigma_z + g_x \cos(\omega_c t)(e^{i\kappa_z \sin(\omega_c t)}\sigma^+ + e^{-i\kappa_z \sin(\omega_c t)}\sigma^-), \quad (S3)$$

where $\dot{U}_1 \equiv \frac{d}{dt}U_1$. Using the Jacoby-Anger identity $e^{\pm i\kappa_z \sin(\omega_c t)} = \sum_{n=-\infty}^{\infty} J_n(\kappa_z)e^{\pm in\omega_c t}$, we can rewrite the Hamiltonian, with use of the Bessel functions of the first kind J_n , in the form

$$H_1/\hbar = \frac{1}{2}\omega_{eg}\sigma_z + \frac{1}{2}g_x (e^{i\omega_c t} + e^{-i\omega_c t}) \sum_{n=-\infty}^{\infty} (J_n(\kappa_z)e^{in\omega_c t}\sigma^+ + J_n(\kappa_z)e^{-in\omega_c t}\sigma^-). \quad (S4)$$

Taking advantage of the Bessel function properties $J_{-n}(x) = (-1)^n J_n(x)$, and $J_{n-1}(x) + J_{n+1}(x) = \frac{2n}{x}J_n(x)$, and splitting the equation into terms with different oscillation frequencies, we rewrite

$$H_1/\hbar = \frac{1}{2}\omega_{eg}\sigma_z + \frac{1}{2}g_x \sum_{n=1}^{\infty} \frac{2n}{\kappa_z} J_n(\kappa_z) (e^{in\omega_c t} + (-1)^{n+1}e^{-in\omega_c t}) \times (\sigma^+ + (-1)^{n+1}\sigma^-). \quad (S5)$$

Note that so far we have not introduced any approximations in the Hamiltonian. In this form, Hamiltonian (S5) separates terms that can be interpreted as n -photon resonances with the effective coupling strengths

$$g_x^{(n)}(\vec{E}_0, \vec{d}_{eg}, \Delta\vec{d}, \omega_c) \equiv g_x^{(n)}(\kappa_z) = \frac{2n}{\kappa_z} J_n(\kappa_z) g_x, \quad (S6)$$

where we have denoted $\Delta\vec{d} = \vec{d}_{ee} - \vec{d}_{gg}$. Hence,

$$H_1/\hbar = \frac{1}{2}\omega_{eg}\sigma_z + \frac{1}{2}g_x^{(1)} (e^{i\omega_c t} + e^{-i\omega_c t}) \sigma_x + \underbrace{\frac{1}{2} \sum_{n=2}^{\infty} g_x^{(n)} (e^{in\omega_c t} + (-1)^{n+1}e^{-in\omega_c t}) \times (\sigma^+ + (-1)^{n+1}\sigma^-)}_{H_{\text{multi}}/\hbar}. \quad (S7)$$

It is worth noticing that the polarity of the system "unlocks" even-photon-number transitions forbidden in inversion-symmetric systems with nonzero d_{eg} . The H_{multi} Hamiltonian gathers all the multiphoton resonance terms.

For the fixed arbitrarily σ_x -coupling strength $g_x/\omega_c = 1$, the values of the couplings as functions of the polarity g_z/g_x of the system are presented illustratively in Fig. S1a. For small PDMs and field amplitudes – typical in optical experiments and calculations – the single photon coupling $g_x^{(1)}$ is dominant. However, highly polarized systems coupled to strong fields may require accounting for higher-order transitions through terms with $n > 1$. Most importantly, as shown in Fig. S1b, for arbitrary and fixed PDMs difference $g_z/g_x = 1$, the coupling strength $g_x^{(1)}$ significantly deviates from standard g_x (dashed line) as we increase the driving field's amplitude g_x/ω_c . This nonlinear behavior is investigated further in the following parts.

In conclusion, transformation U_1 rotates the reference frame sinusoidally in time. The system defined by the Hamiltonian H is described exactly by the Hamiltonian H_1 in the dynamic frame of reference, where resonances at $n\omega_c \approx \omega$, which we will refer to as "higher-order resonances", are explicit.

B. Transformation U_2 – dealing with counter-rotating terms

At this point, the usual step is to disregard the higher-order- and counter-rotating terms in the rotating-wave approximation (RWA). However, the effects at the focus of this work become relevant in strong fields, for which RWA may not be justified. Hence, we are going to incorporate counter-rotating-term corrections following the idea introduced in Ref. [2] by the second unitary transformation

$$U_2 = e^{i\xi\kappa_x \sin(\omega_c t)\sigma_x}, \quad (\text{S8})$$

where $\kappa_x = g_x^{(1)}/\omega_c$. The parameter $\xi \in (0, 1)$ will be evaluated later.

In the frame transformed through U_2 , the inversion operator σ_z acquires terms proportional to the Pauli flip operators in form of $\sigma_y = -i(\sigma^+ - \sigma^-)$, and *vice versa*

$$\begin{aligned} U_2\sigma_zU_2^\dagger &= \cos(2\xi\kappa_x \sin(\omega_c t))\sigma_z + \sin(2\xi\kappa_x \sin(\omega_c t))\sigma_y \\ U_2\sigma_yU_2^\dagger &= \cos(2\xi\kappa_x \sin(\omega_c t))\sigma_y - \sin(2\xi\kappa_x \sin(\omega_c t))\sigma_z. \end{aligned} \quad (\text{S9})$$

We make use of the Bessel expansion once again

$$U_2\sigma_{z,y}U_2^\dagger = \left(J_0(2\xi\kappa_x) + \sum_{k=1}^{\infty} J_{2k}(2\xi\kappa_x) (e^{i2k\omega_c t} + e^{-i2k\omega_c t}) \right) \sigma_{z,y} \mp i \sum_{k=0}^{\infty} J_{2k+1}(2\xi\kappa_x) (e^{i(2k+1)\omega_c t} - e^{-i(2k+1)\omega_c t}) \sigma_{y,z}. \quad (\text{S10})$$

From the form of the expansions we conclude that the rotated Hamiltonian consists of terms with different oscillation frequencies ($\omega_c, 2\omega_c, 3\omega_c, \dots$). The full form reads

$$\begin{aligned} H_2/\hbar &= U_2H_1U_2^\dagger/\hbar + i\dot{U}_2U_2^\dagger = \\ & \frac{1}{2}\omega_{eg} \left[\left(J_0(2\xi\kappa_x) + \sum_{k=1}^{\infty} J_{2k}(2\xi\kappa_x) (e^{i2k\omega_c t} + e^{-i2k\omega_c t}) \right) \sigma_z - i \sum_{2k+1}^{\infty} (2\xi\kappa_x) (e^{i(2k+1)\omega_c t} - e^{-i(2k+1)\omega_c t}) \sigma_y \right] \\ & + \frac{1}{2} \sum_{k=0}^{\infty} g_x^{(2k)}(\kappa_z) (e^{i(2k+1)\omega_c t} + e^{-i(2k+1)\omega_c t}) \sigma_x - \xi g_x^{(1)} \cos(\omega_c t) \sigma_x \\ & + \frac{i}{2} \sum_{k=1}^{\infty} g_x^{2k}(\kappa_z) (e^{i2k\omega_c t} - e^{-i2k\omega_c t}) \times \\ & \left[\left(J_0(2\xi\kappa_x) + \sum_{k=1}^{\infty} J_{2k}(2\xi\kappa_x) (e^{i2k\omega_c t} + e^{-i2k\omega_c t}) \right) \sigma_y + i \sum_{2k+1}^{\infty} (2\xi\kappa_x) (e^{i(2k+1)\omega_c t} - e^{-i(2k+1)\omega_c t}) \sigma_z \right]. \end{aligned} \quad (\text{S11})$$

We separated the different frequency terms in the spirit of the RWA. Keeping time-independent terms and terms oscillating with the frequency ω_c , we arrive at an approximated Hamiltonian relevant for the resonance fluorescence

problem

$$\begin{aligned}
H_2/\hbar \approx & \frac{1}{2} \underbrace{\omega_{eg} J_0(2\xi\kappa_x)}_{\omega'_{eg}} \sigma_z + \underbrace{\sum_{k=1}^{\infty} g_x^{(2k)}(\kappa_z) \frac{4k}{2\xi\kappa_x} J_{2k}(2\xi\kappa_x) \cos(\omega_c t)}_{g'_z} \sigma_z \\
& + \omega_{eg} J_1(2\xi\kappa_x) \sin(\omega_c t) \sigma_y + (1 - \xi) g_x^{(1)}(\kappa_z) \cos(\omega_c t) \sigma_x.
\end{aligned} \tag{S12}$$

Here, we introduced ω'_{eg} , which is the modified resonance frequency shifted due to the influence of the counter-rotating terms. The main contribution to this shift is the well-known Bloch-Siegert shift $\xi^2 (g_x^{(1)})^2 \frac{\omega_{eg}}{\omega_c^2}$, however, the form provided here is more general. We also introduced coupling g'_z which is a correction from the counter-rotating terms to the polar coupling of the system.

At this point, we find the value of the parameter ξ introduced earlier by comparing coupling terms

$$\omega_{eg} J_1(2\xi\kappa_x) = (1 - \xi) g_x^{(1)}(\kappa_z) \equiv \frac{1}{2} \Omega. \tag{S13}$$

This condition simplifies the form of the resulting Hamiltonian and defines the effective coupling strength Ω . After simple transformations, the rewritten Hamiltonian reads

$$H_2/\hbar = \frac{1}{2} \omega'_{eg} \sigma_z + g'_z \cos(\omega_c t) \sigma_z + \frac{1}{2} \Omega (e^{-i\omega_c t} \sigma^+ + e^{i\omega_c t} \sigma^-). \tag{S14}$$

With the second transformation, we have taken into account the counter-rotating terms in the effective parameters ω'_{eg} , g'_z and Ω . We now proceed to effectively remove the σ_z -coupling.

C. Transformation U_3 – effectively removing the σ_z coupling

The above form is very similar to the one given in the initial Hamiltonian (S1). Hence, the oscillating σ_z term can be treated with a transformation analogous to (S2)

$$U_3 = e^{\frac{1}{2} i \kappa'_z \sin(\omega_c t) \sigma_z}, \tag{S15}$$

where $\kappa'_z = g'_z/\omega_c$. The transformed Hamiltonian takes the form which we refer to as Jaynes-Cummings-like since the field is in this case treated classically unlike in the original Jaynes-Cummings model

$$H_3/\hbar \approx \frac{1}{2} \omega'_{eg} \sigma_z + \frac{1}{2} \underbrace{\Omega J_0(\kappa'_z)}_{\Omega'} (e^{-i\omega_c t} \sigma^+ + e^{i\omega_c t} \sigma^-). \tag{S16}$$

Here, Ω' is the effective coupling strength.

D. Transformation U_4 – moving to the interaction picture

Finally, by applying interaction picture transformation

$$U_4 = e^{\frac{1}{2} i \omega_c t \sigma_z}, \tag{S17}$$

and setting effective detuning $\delta' = \omega_c - \omega'_{eg}$, we end up with the final, time-independent form same as Eq. (5) in the main text

$$H_{\text{eff}}/\hbar = -\frac{1}{2} \delta' \sigma_z + \frac{1}{2} \Omega' \sigma_x. \tag{S18}$$

To conclude, we have applied a series of noncommutative unitary transformations or Bloch sphere rotations around the z and x axes. Each of these transformations introduces a Hamiltonian simplification and captures subsequent Hamiltonian terms in effective parameters. As a result, we have arrived at the Hamiltonian H_{eff} , whose simple form captures the rich physics of interactions of light with transition and permanent dipole moments in the ultrastrong coupling regime, including the influence of counter-rotating terms, Bloch-Siegert frequency shift, and beyond. In H_{eff} , we have neglected higher-order resonances of the type $n\omega_c \approx \omega_{eg}$, which is justified with our original assumption that $\omega_c \approx \omega_{eg}$.

II. DERIVATION OF RELAXATION RATE EQ. (7)

To take into account dissipation processes (e.g., spontaneous emission), we consider an additional interaction between the TLS and a bosonic reservoir

$$H_R/\hbar = \sum_p \omega_p b_p^\dagger b_p + \frac{1}{2} \sum_p g_p (b_p^\dagger + b_p) \sigma_x. \quad (\text{S19})$$

The reservoir modes are described by the creation b^\dagger and annihilation b_p operators with corresponding mode frequencies ω_p . The coupling strength between these modes and the system is given by g_p .

We move to the interaction picture for the reservoir by making use of the unitary transformation

$$U_{\text{int}}^R = e^{i \sum_m \omega_m b_m^\dagger b_m t} \quad (\text{S20})$$

that does not affect the system and, therefore, does not interfere with our previous calculations. The interaction-picture Hamiltonian takes the form

$$H_{R,\text{int}}/\hbar = \frac{1}{2} \sum_p g_p (b_p^\dagger e^{i\omega_p t} + b_p e^{-i\omega_p t}) \sigma_x. \quad (\text{S21})$$

We now apply all the transformations U_1 – U_4 to the system operators $\sigma_{x,y,z}$, and list below the nontrivial transformation prescriptions:

$$\begin{aligned} U_1 \sigma_x U_1^\dagger &= \left(J_0(\kappa_z) + \sum_{k=1}^{\infty} J_{2k}(\kappa_z) (e^{i2k\omega_c t} + e^{-i2k\omega_c t}) \right) \sigma_x + \sum_{k=0}^{\infty} J_{2k+1}(\kappa_z) \left(e^{i(2k+1)\omega_c t} - e^{-i(2k+1)\omega_c t} \right) i\sigma_y, \\ U_2 i\sigma_y U_2^\dagger &= \left(J_0(2\xi\kappa_x) + \sum_{k=1}^{\infty} J_{2k}(2\xi\kappa_x) (e^{i2k\omega_c t} + e^{-i2k\omega_c t}) \right) i\sigma_y - \sum_{k=0}^{\infty} J_{2k+1}(2\xi\kappa_x) \left(e^{i(2k+1)\omega_c t} - e^{-i(2k+1)\omega_c t} \right) \sigma_z, \\ U_3 \sigma_1 U_3^\dagger &= \left(J_0(\kappa'_z) + \sum_{k=1}^{\infty} J_{2k}(\kappa'_z) (e^{i2k\omega_c t} + e^{-i2k\omega_c t}) \right) \sigma_1 + \sum_{k=0}^{\infty} J_{2k+1}(\kappa'_z) \left(e^{i(2k+1)\omega_c t} - e^{-i(2k+1)\omega_c t} \right) \sigma_2, \\ U_4 \sigma_x U_4^\dagger &= (\sigma^+ e^{i\omega_c t} + \sigma^- e^{-i\omega_c t}), \\ U_4 i\sigma_y U_4^\dagger &= (\sigma^+ e^{i\omega_c t} - \sigma^- e^{-i\omega_c t}). \end{aligned} \quad (\text{S22})$$

where the third line above applies for pairs $(\sigma_1, \sigma_2) = (\sigma_x, i\sigma_y), (i\sigma_y, \sigma_x)$.

Putting together all the pieces, we end up with a fully transformed Hamiltonian describing system-reservoir inter-

action

$$\begin{aligned}
H_{R,\text{int}}/\hbar &= \frac{1}{2} \sum_p g_p \overline{(b_p^\dagger e^{i\omega_p t} + b_p e^{-i\omega_p t})} \times \\
&\left[- \sum_{k=0}^{\infty} \sum_{l=0}^{\infty} J_{2k+1}(\kappa_z) J_{2l+1}(2\xi\kappa_x) \left(e^{i(2k+1)\omega_c t} - e^{-i(2k+1)\omega_c t} \right) \left(e^{i(2l+1)\omega_c t} - e^{-i(2l+1)\omega_c t} \right) \sigma_z \right. \\
&+ \left[\left(J_0(\kappa_z) + \sum_{k=1}^{\infty} J_{2k}(\kappa_z) \left(e^{i2k\omega_c t} + e^{-i2k\omega_c t} \right) \right) \left(J_0(\kappa'_z) + \sum_{l=1}^{\infty} J_{2l}(\kappa'_z) \left(e^{i2l\omega_c t} + e^{-i2l\omega_c t} \right) \right) \right. \\
&+ \left. \sum_{k=0}^{\infty} J_{2k+1}(\kappa_z) \left(e^{i(2k+1)\omega_c t} - e^{-i(2k+1)\omega_c t} \right) \left(J_0(2\xi\kappa_x) + \sum_{l=1}^{\infty} J_{2l}(2\xi\kappa_x) \left(e^{i2l\omega_c t} + e^{-i2l\omega_c t} \right) \right) \right] \times \\
&\left. \sum_{m=0}^{\infty} J_{2m+1}(\kappa'_z) \left(e^{i(2m+1)\omega_c t} - e^{-i(2m+1)\omega_c t} \right) \right] \frac{(\sigma^+ e^{i\omega_c t} + \sigma^- e^{-i\omega_c t})}{(S23)} \\
&+ \left[\left(J_0(\kappa_z) + \sum_{k=1}^{\infty} J_{2k}(\kappa_z) \left(e^{i2k\omega_c t} + e^{-i2k\omega_c t} \right) \right) \sum_{l=0}^{\infty} J_{2l+1}(\kappa'_z) \left(e^{i(2l+1)\omega_c t} - e^{-i(2l+1)\omega_c t} \right) \right. \\
&+ \left. \sum_{k=0}^{\infty} J_{2k+1}(\kappa_z) \left(e^{i(2k+1)\omega_c t} - e^{-i(2k+1)\omega_c t} \right) \left(J_0(2\xi\kappa_x) + \sum_{l=1}^{\infty} J_{2l}(2\xi\kappa_x) \left(e^{i2l\omega_c t} + e^{-i2l\omega_c t} \right) \right) \right] \times \\
&\left. \left(J_0(\kappa'_z) + \sum_{m=1}^{\infty} J_{2m}(\kappa'_z) \left(e^{i2m\omega_c t} + e^{-i2m\omega_c t} \right) \right) \right] \frac{(\sigma^+ e^{i\omega_c t} - \sigma^- e^{-i\omega_c t})}{(S23)}.
\end{aligned}$$

Since we consider a thermal reservoir in the vacuum state weakly coupled to the system, the terms oscillating at $e^{\pm i(\omega_p - \omega_c)t}$ are significant, while other rapidly oscillating terms in the above equation can be disregarded. Moreover, we can also exclude the whole second rectangular bracket, as all the multiplications provide time-dependent terms. Hence, the complexity of the problem reduces significantly and we arrive at

$$H_{R,\text{int}}/\hbar \approx \frac{1}{2} \sum_p g_p \alpha \left(b_p^\dagger \sigma^- e^{i(\omega_p - \omega_c)t} + b_p \sigma^+ e^{-i(\omega_p - \omega_c)t} \right), \quad (S24)$$

with

$$\begin{aligned}
\alpha(\kappa_z, \kappa_x, \kappa'_z) &= J_0(\kappa_z) J_0(\kappa'_z) + 2 \sum_{k=1}^{\infty} J_{2k}(\kappa_z) J_{2k}(\kappa'_z) - 2 J_0(2\xi\kappa_x) \sum_{k=0}^{\infty} J_{2k+1}(\kappa_z) J_{2k+1}(\kappa'_z) \\
&- 2 \sum_{k=0}^{\infty} \sum_{l=1}^{\infty} J_{2k+1}(\kappa_z) J_{2l}(2\xi\kappa_x) J_{2(k+l)+1}(\kappa'_z) + 2 \sum_{k=0}^{\infty} \sum_{m=0}^{\infty} J_{2k+1}(\kappa_z) J_{2(k+m+1)}(2\xi\kappa_x) J_{2m+1}(\kappa'_z) \quad (S25) \\
&- 2 \sum_{l=1}^{\infty} \sum_{m=0}^{\infty} J_{2(l+m)+1}(\kappa_z) J_{2l}(2\xi\kappa_x) J_{2m+1}(\kappa'_z).
\end{aligned}$$

Following the Weisskopf-Wigner theory [3], we find the effective spontaneous emission rate to be the same as Eq. (7) from the main text

$$\gamma' = \alpha^2 \gamma \approx (J_0(\kappa_z) J_0(\kappa'_z))^2 \gamma, \quad (S26)$$

where γ is the emission rate for the non-polar case. Note that in the resulting frame, due to the PDMs, the effective spontaneous emission rate becomes dependent on the external field amplitude \vec{E}_0 . The emission rate keeps its original value γ without PDMs or the external field. The result given by Eq. (S26) without the approximation is presented graphically in the main text in Fig. 1d. The appearance of the PDMs in the system significantly reduces the gamma rate, while strong field interaction incorporates small correction (compare the blue and orange curves).

III. STATIONARY SOLUTION

Based on the above expressions, we can write the master equation for the polar system's density matrix ρ which also undergoes the unitary transformations

$$\rho \rightarrow U_4(t)U_3(t)U_2(t)U_1(t)\rho U_1^\dagger(t)U_2^\dagger(t)U_3^\dagger(t)U_4^\dagger(t) \quad (\text{S27})$$

under the evolution of the approximated Hamiltonian Eq. (S18)

$$\dot{\rho} = [H_{\text{eff}}/\hbar, \rho] - i\frac{\gamma'}{2} (\sigma^+ \sigma^- \rho + \rho \sigma^+ \sigma^- - 2\sigma^- \rho \sigma^+). \quad (\text{S28})$$

To solve this equation for the stationary state ($\dot{\rho}(t) = 0$), we rewrite it in the matrix form for the expectation values of the operators σ_z, σ^\pm

$$\vec{0} = \begin{pmatrix} -i\delta' - \frac{1}{2}\gamma' & 0 & -\frac{1}{2}i\Omega' \\ 0 & i\delta' - \frac{1}{2}\gamma' & \frac{1}{2}i\Omega' \\ -i\Omega' & i\Omega' & -\gamma' \end{pmatrix} \begin{pmatrix} \langle \sigma^+ \rangle_s \\ \langle \sigma^- \rangle_s \\ \langle \sigma_z \rangle_s \end{pmatrix} - \begin{pmatrix} 0 \\ 0 \\ \gamma' \end{pmatrix}, \quad (\text{S29})$$

where subscript s indicates stationary solution

$$\begin{aligned} \langle \sigma^\pm \rangle_s &= \frac{\Omega'(2\delta' \pm i\gamma')}{2\Omega'^2 + 4\delta'^2 + \gamma'^2}, \\ \langle \sigma_z \rangle_s &= -\frac{(4\delta'^2 + \gamma'^2)}{2\Omega'^2 + 4\delta'^2 + \gamma'^2}. \end{aligned} \quad (\text{S30})$$

IV. FLUORESCENCE SPECTRA

The general formula for the emission spectrum reads [3]

$$S(\omega) = \frac{1}{2\pi} \lim_{T \rightarrow \infty} \frac{1}{T} \int_0^T dt \int_0^T dt' g^{(1)}(t, t') e^{-i\omega(t-t')}, \quad (\text{S31})$$

where $g^{(1)}$ is the first-order correlation function

$$g^{(1)}(t, t') = \langle U^\dagger(t)\sigma^+U(t)U^\dagger(t')\sigma^-U(t') \rangle, \quad (\text{S32})$$

where $U(t)$ is an evolution operator of Hamiltonian Eq. (S1). The further calculations in this section provide generalization of the work done in Ref. [2]. The correlation function can be found analytically in the reference frame rotated according to the sequence of operators U_1-U_4

$$\begin{aligned} \sigma^\pm &\rightarrow U_4(t)U_3(t)U_2(t)U_1(t)\sigma^\pm U_1^\dagger(t)U_2^\dagger(t)U_3^\dagger(t)U_4^\dagger(t) \\ &= \frac{1}{2} \sum_{m \text{ odd}}^\infty (j'_{m+1} e^{\pm im\omega_c t} + j_{m+1} e^{\mp im\omega_c t}) \sigma_z \\ &\quad + \frac{1}{2} \sum_{m=0}^\infty [(\alpha_m e^{\pm im\omega_c t} + \beta_m e^{\mp im\omega_c t}) \sigma^\pm + (\alpha'_m e^{\pm im\omega_c t} + \beta'_m e^{\mp im\omega_c t}) \sigma^\mp], \end{aligned} \quad (\text{S33})$$

where the σ^\pm operators on the right-hand side are given in the rotated reference frame. Above, we have used the following symbols

$$\begin{aligned} j_n &= \begin{cases} 1 + J_0(2\xi\kappa_x), & n = 1 \\ J_{n-1}(2\xi\kappa_x), & n \neq 1 \end{cases} \\ j'_n &= \begin{cases} 1 - J_0(2\xi\kappa_x), & n = 1 \\ -J_{n-1}(2\xi\kappa_x), & n \neq 1 \end{cases} \end{aligned} \quad (\text{S34})$$

and

$$\alpha_m = \begin{cases} \frac{1}{2} \sum_{n \text{ odd}}^{\infty} J_n(\kappa_z^\Sigma)(j_{n+2} - j_n), & m = 0 \\ J_0(\kappa_z^\Sigma)j_1 + \sum_{n \text{ odd}}^{\infty} [J_{n+1}(\kappa_z^\Sigma)j_{n+2} + J_{n-1}(\kappa_z^\Sigma)j_n], & m = 1 \\ \sum_{n \text{ odd}}^{\infty} [J_{m-n}(\kappa_z^\Sigma)j_n + J_{m+n}(\kappa_z^\Sigma)j_{n+2} - J_{n-m}(\kappa_z^\Sigma)j_n], & m \text{ even} \\ \sum_{n \text{ odd}}^{\infty} [J_{m-n}(\kappa_z^\Sigma)j_n + J_{m+n}(\kappa_z^\Sigma)j_{n+2} + J_{n-m}(\kappa_z^\Sigma)j_n] + J_0(\kappa_z^\Sigma)j_m, & m \text{ odd} \end{cases} \quad (\text{S35})$$

$$\beta_m = \begin{cases} \frac{1}{2} \sum_{n \text{ odd}}^{\infty} J_n(\kappa_z^\Sigma)(j_{n+2} - j_n), & m = 0 \\ J_0(\kappa_z^\Sigma)j_{1+2} + \sum_{n \text{ odd}}^{\infty} [J_{n+1}(\kappa_z^\Sigma)j_n + J_{n-1}(\kappa_z^\Sigma)j_{n+2}], & m = 1 \\ - \sum_{n \text{ odd}}^{\infty} [J_{m-n}(\kappa_z^\Sigma)j_{n+2} + J_{m+n}(\kappa_z^\Sigma)j_n - J_{n-m}(\kappa_z^\Sigma)j_{n+2}], & m \text{ even} \\ \sum_{n \text{ odd}}^{\infty} [J_{m-n}(\kappa_z^\Sigma)j_{n+2} + J_{m+n}(\kappa_z^\Sigma)j_n + J_{n-m}(\kappa_z^\Sigma)j_{n+2}] + J_0(\kappa_z^\Sigma)j_{m+2}. & m \text{ odd} \end{cases} \quad (\text{S36})$$

The relation between the primed and non-primed parameters is

$$\alpha_m, \beta_m \xrightarrow[\substack{j_n \rightarrow j'_n \\ j_{n+2} \rightarrow j'_n \\ \kappa_z^\Sigma \rightarrow \kappa_z^\Delta}]{\quad} \alpha'_m, \beta'_m. \quad (\text{S37})$$

Above, $\kappa_z^\Sigma = \kappa_z + \kappa'_z$, and $\kappa_z^\Delta = \kappa_z - \kappa'_z$.

Eventually, the correlation function reads as

$$\begin{aligned} g^{(1)}(t, t') = & \left\langle \left(\frac{1}{2} \sum_{m' \text{ odd}}^{\infty} (j'_{m'+1} e^{im'\omega_c t} + j_{m'+1} e^{-im'\omega_c t}) \sigma_z \right. \right. \\ & + \frac{1}{2} \sum_{m'=0}^{\infty} \left[(\alpha_{m'} e^{im'\omega_c t} + \beta_{m'} e^{-im'\omega_c t}) \sigma^+ + (\alpha'_{m'} e^{im'\omega_c t} + \beta'_{m'} e^{-im'\omega_c t}) \sigma^- \right] \\ & \times \left(\frac{1}{2} \sum_{m \text{ odd}}^{\infty} (j'_{m+1} e^{-im\omega_c t'} + j_{m+1} e^{im\omega_c t'}) \sigma_z \right. \\ & \left. \left. + \frac{1}{2} \sum_{m=0}^{\infty} \left[(\alpha_m e^{-im\omega_c t'} + \beta_m e^{im\omega_c t'}) \sigma^- + (\alpha'_m e^{-im\omega_c t'} + \beta'_m e^{im\omega_c t'}) \sigma^+ \right] \right) \right\rangle. \end{aligned} \quad (\text{S38})$$

We have obtained an expression with two types of terms with exponents: $e^{\pm im'\omega_c t} e^{\mp im\omega_c t'}$, and $e^{\pm im'\omega_c t} e^{\pm im\omega_c t'}$. To calculate the spectrum based on Eq. (S31), we integrate each of these terms, approximating as follows

$$\begin{aligned} I(\omega) = & \lim_{T \rightarrow \infty} \frac{1}{T} \int_0^T dt \int_0^T dt' e^{\pm im'\omega_c t} e^{\mp im\omega_c t'} e^{-i\omega(t-t')} \langle \sigma_\mu(t-t') \sigma_\nu(0) \rangle \\ = & \lim_{T \rightarrow \infty} \frac{1}{T} \int_0^T dt' e^{\pm i(m'-m)\omega_c t'} \int_{-t'}^{T-t'} d\tau e^{\pm i(m'\omega_c \mp \omega)\tau} \langle \sigma_\mu(\tau) \sigma_\nu(0) \rangle \\ \approx & \delta_{m',m} \int_{-\infty}^{\infty} d\tau e^{\pm i(m'\omega_c \mp \omega)\tau} \langle \sigma_\mu(\tau) \sigma_\nu(0) \rangle_s, \end{aligned} \quad (\text{S39})$$

where $\tau = t - t'$, $\mu, \nu \in \{z, +, -\}$ and we moved to the stationary state for the expectation values $\langle \sigma_\mu(\tau) \sigma_\nu(0) \rangle \rightarrow \langle \sigma_\mu(\tau) \sigma_\nu(0) \rangle_s$ by setting integral limits $T - t' \rightarrow \infty$, $-t' \rightarrow -\infty$. Due to this approximation, we simplified the

correlation function by removing one of the sums, as only the terms with $m = m'$ contribute. Moreover, following the same procedure for terms $e^{\pm im' \omega_c t} e^{\pm im \omega_c t'}$, we end up with $\delta_{m', -m}$ which leaves only one term with $m' = -m = 0$, as $m, m' \geq 0$.

We end up with a compact form of the expression for the fluorescence spectrum

$$S(\omega) = \frac{1}{4\pi} \text{Re} \int_0^\infty d\tau \sum_{n=0}^\infty \sum_{\mu, \nu} (A_{\mu\nu}^+(n) e^{i\omega_c \tau} + A_{\mu\nu}^-(n) e^{-i\omega_c \tau}) \times \langle \sigma_\mu(\tau) \sigma_\nu(0) \rangle, \quad (\text{S40})$$

where

$$\begin{aligned} A_{zz}^+(n) &= \begin{cases} 0, & n \text{ even} \\ j'_{n+1}{}^2, & n \text{ odd} \end{cases} \\ A_{z-}^+(n) = A_{+z}^+(n) &= \begin{cases} 0, & n \text{ even} \\ j'_{n+1} \alpha_n, & n \text{ odd} \end{cases} \\ A_{z+}^+(n) = A_{-z}^+(n) &= \begin{cases} 0, & n \text{ even} \\ j'_{n+1} \alpha'_n, & n \text{ odd} \end{cases} \\ A_{--}^+(n) = A_{++}^+(n) &= \begin{cases} \alpha_n \alpha'_n + \alpha'_n \beta_n, & n = 0 \\ \alpha_n \alpha'_n, & n \neq 0 \end{cases} \\ A_{-+}^+(n) &= \begin{cases} \alpha_n^2 + \alpha'_n \beta'_n, & n = 0 \\ \alpha_n^2, & n \neq 0 \end{cases} \\ A_{+-}^+(n) &= \begin{cases} \alpha_n^2 + \alpha_n \beta_n, & n = 0 \\ \alpha_n^2, & n \neq 0 \end{cases} \\ A_{\mu\nu}^+(n) &\xrightarrow[\substack{j'_n \rightarrow j_n \\ \alpha_n, \alpha'_n \rightarrow \beta_n, \beta'_n \\ \beta_n, \beta'_n \rightarrow \alpha_n, \alpha'_n}]{\hspace{1.5cm}} A_{\mu\nu}^-(n). \end{aligned} \quad (\text{S41})$$

Finally, we evaluate the expectation values for the operators. We are interested in the incoherent part of the spectrum, hence, we use the quantity

$$\langle \langle \sigma_\mu(\tau) \sigma_\nu(0) \rangle \rangle = \langle \sigma_\mu(\tau) \sigma_\nu(0) \rangle_s - \langle \sigma_\mu \rangle_s \langle \sigma_\nu \rangle_s. \quad (\text{S42})$$

Using the quantum regression theorem [3] and following reasoning in Ref. [2] for the master equation Eq. (S28), we find that

$$\frac{d}{d\tau} \langle \langle \sigma_\mu(\tau) \sigma_\nu(0) \rangle \rangle = \sum_\lambda M_{\mu\lambda} \langle \langle \sigma_\lambda(\tau) \sigma_\nu(0) \rangle \rangle, \quad (\text{S43})$$

where M is the matrix responsible for the homogeneous evolution in the GKLS equation (S29)

$$M = \begin{pmatrix} -i\delta' - \frac{1}{2}\gamma' & 0 & -\frac{1}{2}i\Omega' \\ 0 & i\delta' - \frac{1}{2}\gamma' & \frac{1}{2}i\Omega' \\ -i\Omega' & i\Omega' & -\gamma' \end{pmatrix}. \quad (\text{S44})$$

Making use of the Laplace transformation $\mathcal{L}(f(t)) = \int_0^\infty f(t) e^{-s\tau} d\tau = \mathcal{L}[f](s)$, this set of equations can be written as

$$\left(M - \frac{1}{s} I \right) \mathcal{L}[X_\nu](s) = X_{0\nu}, \quad (\text{S45})$$

where $X_{0\nu}$ provides initial conditions

$$X_{0\nu} = \begin{pmatrix} \langle \langle \sigma^+(0) \sigma_\nu(0) \rangle \rangle \\ \langle \langle \sigma^-(0) \sigma_\nu(0) \rangle \rangle \\ \langle \langle \sigma_z(0) \sigma_\nu(0) \rangle \rangle \end{pmatrix}, \quad X_\nu = \begin{pmatrix} \langle \langle \sigma^+(\tau) \sigma_\nu(0) \rangle \rangle \\ \langle \langle \sigma^-(\tau) \sigma_\nu(0) \rangle \rangle \\ \langle \langle \sigma_z(\tau) \sigma_\nu(0) \rangle \rangle \end{pmatrix}. \quad (\text{S46})$$

The solutions can be expressed as [2]

$$\langle\langle\sigma_\mu(\tau)\sigma_\nu(0)\rangle\rangle = \sum_{l=1}^3 R_{\mu\nu}^l e^{s_l \tau} \quad (\text{S47})$$

where $R_{\mu\nu}^l = \lim_{s \rightarrow s_l} (s - s_l) \mathcal{L}[\langle\langle\sigma_\mu(\tau)\sigma_\nu(0)\rangle\rangle](s)$, for s_l being the roots of the determinant

$$\det\left(M - \frac{1}{s}I\right) = s^3 + 2\gamma' s^2 + (\Omega'^2 + \delta'^2 + \frac{5}{4}\gamma'^2)s + \gamma'(\frac{1}{2}\Omega'^2 + \delta'^2 + \frac{1}{4}\gamma'^2), \quad (\text{S48})$$

which are of the form $s_1 = -\gamma_1$, $s_2 = -\gamma_2 + i\tilde{\Omega}$, $s_3 = -\gamma_2 - i\tilde{\Omega}$, and $\gamma_{1,2}, \tilde{\Omega} \geq 0$.

Hence, the spectrum can be written as

$$S(\omega) = \frac{1}{4\pi} \text{Re} \sum_{n=0}^{\infty} \sum_{\mu,\nu} \sum_{l=1}^3 \left[A_{\mu\nu}^+(n) R_{\mu\nu}^l \int_0^{\infty} d\tau e^{-i(\omega - n\omega_c)\tau + s_l \tau} + A_{\mu\nu}^-(n) R_{\mu\nu}^l \int_0^{\infty} d\tau e^{-i(\omega + n\omega_c)\tau + s_l \tau} \right], \quad (\text{S49})$$

With that, we can calculate the above integrals which describe the lineshapes $L_{n,l}^\pm(\omega)$

$$L_{n,l}^\pm(\omega) = \begin{cases} \frac{\gamma_1 - i(\omega \mp n\omega_c)}{\gamma_1^2 + (\omega \mp n\omega_c)^2}, & l = 1 \\ \frac{\gamma_2 - i(\omega \mp n\omega_c - \tilde{\Omega})}{\gamma_2^2 + (\omega \mp n\omega_c - \tilde{\Omega})^2}, & l = 2 \\ \frac{\gamma_2 - i(\omega \mp n\omega_c + \tilde{\Omega})}{\gamma_2^2 + (\omega \mp n\omega_c + \tilde{\Omega})^2}, & l = 3. \end{cases} \quad (\text{S50})$$

Lineshape intensities $I_{n,l}^\pm$ are given by

$$I_{n,l}^\pm = \sum_{\mu,\nu} A_{\mu\nu}^\pm(n) R_{\mu\nu}^l. \quad (\text{S51})$$

Finally, the full spectrum can be calculated as

$$S(\omega) = \frac{1}{4\pi} \sum_{n=0}^{\infty} \sum_{l=1}^3 \left(I_{n,l}^+ L_{n,l}^+(\omega) + I_{n,l}^- L_{n,l}^-(\omega) \right). \quad (\text{S52})$$

- [1] O. Kibis, G. Y. Slepyan, S. Maksimenko, and A. Hoffmann, Matter coupling to strong electromagnetic fields in two-level quantum systems with broken inversion symmetry, *Physical review letters* **102**, 023601 (2009).
 [2] Y. Yan, Z. Lü, and H. Zheng, Effects of counter-rotating-wave terms of the driving field on the spectrum of resonance fluorescence, *Physical Review A—Atomic, Molecular, and Optical Physics* **88**, 053821 (2013).
 [3] M. O. Scully and M. S. Zubairy, *Quantum optics* (Cambridge university press, 1997).